

Initial cellular response to laser surface engineered biomaterials

Ljupcho Prodanov, Edwin Lamers, X. Frank Walboomers, and John A. Jansen

Introducing micro- and nanoscale features on biomaterials in an engineered, controlled manner has been shown to positively affect medical implant integration into the human body. A key factor in this process is the initial cellular response toward the implant. Different techniques such as chemical treatment, plasma spraying, lithography, and coatings, among others, have been applied during the last decades to improve the implant integration. One of the methods that started to be recently exploited is laser surface engineering (LSE). LSE offers a wide range of new surface engineering methods, such as laser surface melting (LSM), laser engineered net shaping (LENS), and selective laser melting/sintering (SLM/S) that can generate complex micro- and nanoscale features with high resolution. This review provides an overview of the initial cellular response to medical implants and the different techniques used to modify the surface of different biomaterials. An emphasis is given to laser techniques that were recently developed for surface texturing, describing *in vitro*, pre-clinical, and clinical trials performed thus far.

Introduction

Materials that can replace part of a living structure or biofunction are called "biomaterials" and have been widely used for dental implants, hip implants, plastic surgery, heart valves, and cardiac pacemakers.[1,2] The typical size of a cell is 10–20 μm, whereas the characteristic dimensions of cell surface structures (receptors, filopodia, and lamelopodia) that interact with biomaterials or the extracellular matrix (ECM) are in the order of a few nanometers.[3] Thus, by introducing microscale or nanoscale topography on biomaterials without compromising the material properties, researchers want to achieve better cellular attachment. In this way, the integration of an implant into bone or other tissues can be improved. Indeed, it is very important that the implanted material integrates in the surrounding tissue and is functional in the living tissue; in other words, the implant should be "biocompatible."

Introducing surfaces containing micro- and nanoscale features in an engineered controlled manner has already been shown to significantly affect medical implant integration into the human body.[4] A key factor in this process is the initial cellular response toward the device; and to improve this interaction, different techniques such as chemical treatment, plasma spraying, sputtering, lithography, and organic or inorganic coatings have been applied alone or in different combinations.[5] One of the methods that has started to be exploited recently is laser surface engineering because of its precision, speed, and an optimal price-performance ratio.

This review describes how lasers are used to modify and enhance surface properties of biomaterials. To get a better understanding of these processes, we first discuss the relevant processes that occur at the implant interface, and then provide a short overview of different techniques used to modify the surface topography. Subsequently, we will specifically focus on the laser techniques that have been developed for surface texturing by describing *in vitro*, pre-clinical, and clinical trials for bone tissue replacement. Finally, we will discuss the advantages and disadvantages of laser surface engineering.

Interface and initial events

The success of bone as well as other implants depends on better cell-material interactions as it improves the fixation of an implant into the tissue. The process of implant integration into a tissue is complex in nature, and depending on the biocompatibility of the implant, it can lead to different final outcomes, which

Ljupcho Prodanov, Radboud University Nijmegen Medical Center; L.Prodanov@dent.umcn.nl
Edwin Lamers, Radboud University Nijmegen Medical Center; e.lamers@dent.umcn.nl
X. Frank Walboomers, Radboud University Nijmegen Medical Center; f.walboomers@dent.umcn.nl
John A. Jansen, Radboud University Nijmegen Medical Center; j.jansen@dent.umcn.nl
DOI: 10.1557/mrs.2011.273

© 2011 Materials Research Society
https://doi.org/10.1557/mrs.2011.273 Published online by Cambridge University Press

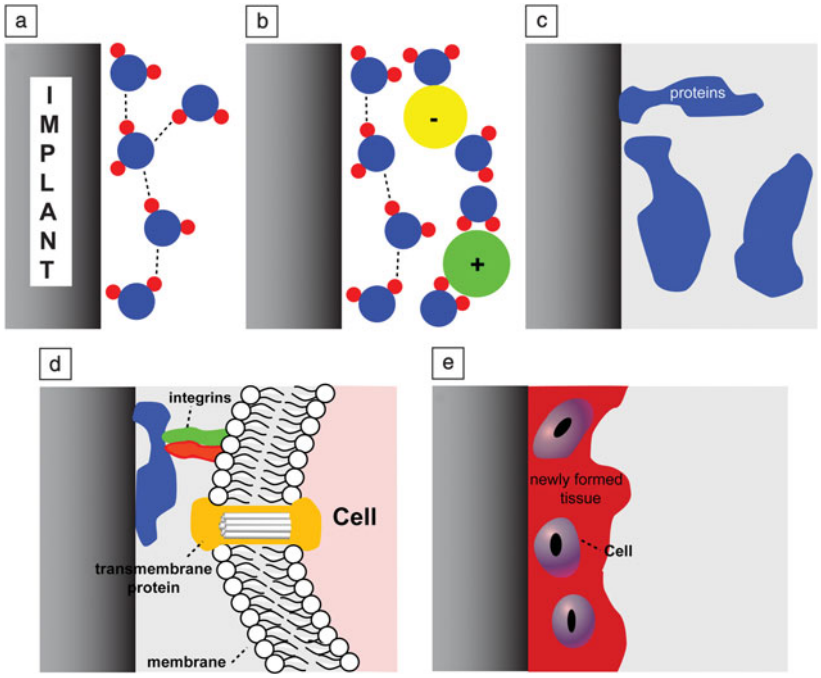


Figure 1. Initial processes on the interface between a biomaterial and biofluid immediately after implantation. (a) The surface is first exposed to water, and the interactions are strongly affected by the surface free energy of the implant surface. (b) The surface is covered with a layer of hydrated ions followed by proteins (c). (d) Interaction of blood cells with the implant surface via cell receptor integrins. (e) Regenerated tissue at the implant-tissue interface.

result in either full integration or implant loss.[6] When looking at initial stages immediately after the placement of an implant into a freshly prepared surgical site, water, ions, and serum proteins arrive at the biomaterial surface (**Figure 1**). An important parameter for the adhesion of these molecules is the surface free energy (or wettability) of an implant surface, which is reflected by its hydrophilicity.[7] Differences in surface wettability (e.g., very hydrophilic or hydrophobic) provide different opportunities for protein binding. Generally, the more hydrophilic a surface, the more proteins will be adsorbed.

Directly after the adherence of proteins on the implant site, monocytes arrive (blood cells involved in immune response). If these cells adhere to the implant, they can mature into macrophages (**Figure 2**). Macrophages are the key orchestrator in the inflammation process and produce a large number of biologically active products such as proteases, coagulation factors, growth factors, and cytokines (proteins that regulate immune response). These processes trigger different events around the implant, greatly determining whether an implantation will clinically succeed.[8] Degradable implants usually are resorbed in time by macrophages. After resorption, a fibrotic tissue (scar) will remain. The most common unwanted process that occurs at the implant site is encapsulation of the implant.[6] If this occurs, macrophages will fuse to form giant cells to enhance their effectiveness. The giant cells will start releasing signals to attract connective cells (fibroblasts) from the surrounding tissue.[9] Fibroblasts and vascular endothelial cells will form granulation tissue and encapsulate the implant with a thin layer of collagenous matrix to isolate the implant from the surrounding tissue.[10] The formation of this collagen matrix layer is often called the "foreign body reaction."[8]

If cells from the tissue surrounding the replacement (bone cells) are attached to the adhered proteins on the surface of the biomaterial, the implant can be integrated directly into the surrounding tissue without the formation of a fibrous capsule. This response is frequently described for bone tissue as osseointegration. During this event, platelets and macrophages start secreting proteins for bone regeneration (transforming growth factor beta [TGF-β], bone morphogenetic protein [BMP], and platelet derived growth factor [PDGF]) that will adhere to the provisional matrix. The presence of these proteins at the implant surface induces the interaction between bone cells and the protein loaded implant, which is ultimately followed by tissue regeneration at the implant site. Bone formed at the implant surface is considered a positive result, whereas fibrous encapsulation is considered a negative result.[11]

Biomaterial properties

Bulk composition, mechanical characteristics, and surface properties such as surface free energy, surface charge, ion release

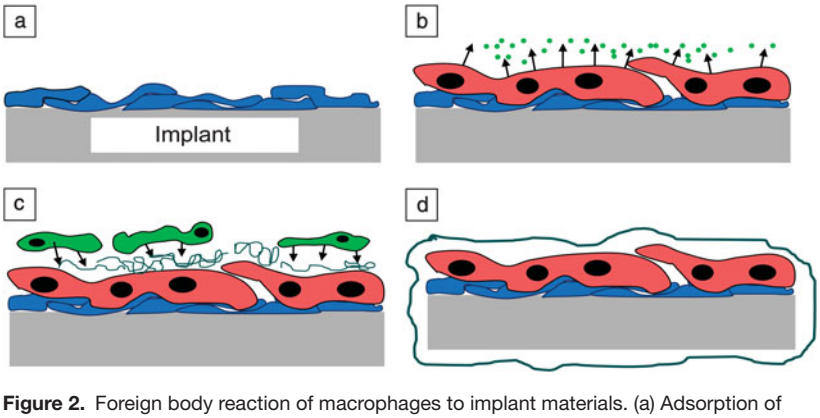


Figure 2. Foreign body reaction of macrophages to implant materials. (a) Adsorption of plasma proteins (blue). (b) Macrophages attached to the implant site fuse into giant cells (red) releasing digestive molecules (green). (c) The giant cells start releasing chemotactic factors to attract collagen-secreting (dark green) fibroblasts (green). (d) Collagenous matrix proteins are released, and the implant is encapsulated (dark green).

https://doi.org/10.1557/mrs.2011.273 Published online by Cambridge University Press

(not discussed in this review), and perhaps even more importantly the specific surface topography of a material, determine the wound healing response and tissue repair after implantation. Micrometer and nanometer roughness first enhance the hydrophilicity of a material when compared to its smooth counterpart.[12] The importance of surface topography has already been recognized on many levels for a long time.[13–15] Biological systems recognize and respond to the surface through surface patterns. Implant surfaces are thus rarely smooth but generally have a certain topography, which can be either roughness (a specific topography) or texture (structured topography).[16] Surface roughness is characterized by randomly distributed surface topographies, whereas surface texture is characterized by a regular surface topography with defined dimensions and distribution. Surface topography can be divided into three levels: macro-, micro-, and nano-sized topologies. Macro-sized topography (>100 μm; **Figure 3**a) improves mechanical stability; however, it also introduces an increased risk of the induction of inflammatory processes.[17] Microscale surface topography (1–100 μm; Figure 3b) maximizes the interlocking between ingrowth of mineralized bone and the implant surface. An advantage of micro-sized roughness is the early bone implant contact, which is especially important in patients with insufficient bone quantity or anatomical limitations. Nanoscale surface topography (<100 nm; Figure 3c) is least understood, yet it falls in the same order of size as the natural ECM, and it seems ultimately important to determine the adsorption of proteins, the adhesion of bone cells (osteoblasts), and rate of bone healing.[18] The ECM contains mostly collagen Type I fibrils that have a diameter of 1.4 nm, a length of 300 nm, and are staggered with a periodicity of 68 nm. Additionally, compact bone has an average roughness of 32 nm, which is also in the nanometer scale.[19] Mimicking such dimensions of the ECM on implant biomaterials by the use of nanotechnology might improve bone healing after implantation.

Non-laser techniques used to modify the surface topography

It is important to emphasize that prior to the use of lasers for surface modification of biomaterials, a variety of techniques for random and ordered topographies were developed. The role that the micro- and nanoscale topography of a surface can play in controlling cell responses has been well documented and has led to an interest in studying cell response to submicron-scale surface features.

Random micro- and nano-roughness

Random micro- and nano-roughness can be created by several techniques, such as machining,[20] chemical (acid) etching, anodization,[21–23] sintering,[24] self-assembly,[25] and polymer demixing.[26,27] Substrates created with such techniques display a completely random micro- and nano-roughness. The formed pattern dimensions are dependent on acid concentration and composition, current, electrolyte temperature, and time of incubation.

Ordered micro- and nano-texture

Manifold lithographic techniques[28] have been used to create textured surfaces with ordered micro- and nano-roughness. Electron beam lithography (EBL),[27,29] focused ion beam processing (FIBP),[30,31] nanocontact printing (NP),[32] and nanoimprint lithography (NIL)[33,34] are widely used for this purpose, and surface features down to 5 nm can be created. The general setup for all lithographic techniques is that they require spin coaters, vacuum chambers, and optimization protocols to coat and develop specific photoresists or thin films, and they are time-consuming.

In vitro *studies using nanotopography*

The groups of Jansen,[35] Curtis,[36] and Dalby[37] were the pioneers in the field of surface texturing and performed *in vitro* studies on substrates bearing several different microtopographical (semi-) ordered patterns (pits, pillars, and grooves). More recently, several studies demonstrated the beneficial effects of nanophase materials compared to conventional materials on osteoblast adhesion, proliferation, and differentiation.[24,38–44] Dalby et al.[45–50] performed many studies on nano-sized islands. Such islands can be formed using spontaneous mixing of two polymers (polystyrene and poly(4-bromostyrene)), with the height of the features determined by the polymer concentration. Results demonstrated that fibroblast and endothelial cell adhesion and focal adhesion formation were mostly enhanced on islands with dimensions around 10–13 nm. In addition, studies of osteoblast behavior on polymer demixed islands demonstrated that spreading and differentiation were specifically enhanced on 10 nm high islands.[51]

Thus far, several types of nanotextures created with EBL have been used for cell culture assays, such as pits, pillars, and grooves. First Curtis et al.[36] and later Dalby and Biggs et al.[49,55–59] used large arrays of pits or pillars in silicon with a diameter of 120 nm or less and a center-to-center spacing of 300 nm or

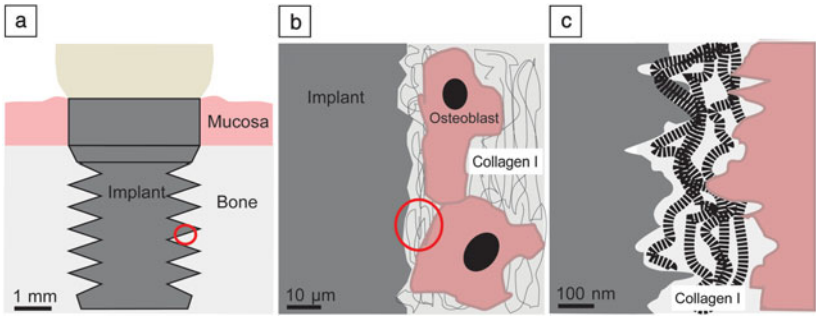


Figure 3. Overview of several topographies on a dental implant ranging from (a) macroscale (i.e., >100 μm), (b) microscale (1–100 μm), and down to (c) nanoscale (<100 nm).

https://doi.org/10.1557/mrs.2011.273 Published online by Cambridge University Press

less. Using an optimized method of EBL, 1 × 1 cm^2 areas were created within one hour. These were used as a master for replication into either polymethylmethacrylate (PMMA), poly(caprolactone) (PCL), or (poly)carbonate (PC). Using the nanopatterned replicas, Dalby et al. demonstrated that the 13-nm islands produced fibroblasts with the biggest area, and 95 nm islands produced cells with the smallest areas.[49] Loesberg et al.[60] studied fibroblast alignment on a polystyrene "biochip" containing 50 different nanotextured patterns in a range of groove dimensions, nanopits, and squares. The study showed that fibroblasts sense patterns with a feature size down to 35 nm. Recently, we studied initial osteoblast behavior on the same substrates and demonstrated that osteoblasts are more sensitive to nanopatterns than fibroblasts and respond to patterns with a feature size down to 18 nm. The same study also demonstrated that groove depth and width are key factors in determining the osteoblast response and calcium formation by osteoblasts.[61]

Finally, nanocontact printing experiments on both micro- and nanoscale (protein) patterns have been performed to study the behavior of cells (i.e., neuronal, melanoma, and capillary endothelial cells). Patterns influenced many cellular processes, such as motility, adhesion, spreading, and differentiation.[62–66]

In vivo *studies using techniques excluding laser treatment*

Only preliminary studies have been reported assessing the biocompatibility of nanotextured biomaterials *in vivo*. Giavaresi et al. studied the effect of polymeric nanopits and nanocylinders on fibrous capsule formation and vascularity by implanting the biomaterials subcutaneously into rats. The study demonstrated that nanopits increased the development of fibrous capsules, while nanocylinders increased the cellularity of the fibrous capsule and the vascular density.[67]

In another *in vivo* study, Popat et al. first studied the *in vivo* biocompatibility of nanotubular substrates with a pore size of approximately 80 nm by subcutaneous implantation of the biomaterial into rats. The study demonstrated that TiO_2 nanotubular substrates did not induce fibrous tissue formation around the implant and concluded that the biomaterials were biocompatible.[68]

Laser surface engineering

LSE is a material processing method to melt, heat, or modify the surface of different types of materials. In general, the laser beam is focused to a small spot and has a power density that is sufficiently high for the material to absorb it, rather than reflect it. Briefly, lasers are devices that transform light of varying frequencies into a single intensity in the infrared, visible, ultraviolet, or x-ray regions of the spectrum and can be based on liquids, gases, solid-state materials, and excimers.[69–72]

For texturing applications, various lasers are used depending on the features to be fabricated and the type of material to be processed. Most of the *in vitro* studies on cell-implant interactions applied the laser surface melting (LSM) technique with neodymium doped yttrium aluminium garnet (Nd:YAG) or CO_2 lasers or used excimer lasers for ablation. The actions of CO_2 and Nd:YAG lasers are generally thermal processes, whereas the actions of the different excimer lasers produce almost no heat.[73] In this section, the potential of LSE using laser texturing methods will be described.

Lasers surface melting

Generally in LSM, a thin surface layer is rapidly melted by a predetermined energy density laser beam into a focused spot on the surface, followed by rapid ablation and solidification to produce a microstructure. Usually the laser is used in a continuous wave, meaning that its output is nominally constant over an interval of seconds or longer. Prior to ablation of the material, the absorption of radiation at the surface raises its temperature, and this results in melting at the surface. As the temperature continues to rise, vaporization of the material occurs, and finally it solidifies when the temperature drops, leaving a patterned surface behind.[74] Thus, melting, evaporation, and solidification are the series of steps involved in generation of new surface topography, and the rapid cooling rate results in homogenization and the refinement of microstructures or nanostructures. The beam from a Nd:YAG laser can be focused to a smaller spot size because of shorter wavelength compared to a CO_2 laser.

Laser engineered net shaping

The LENS process uses metal powders that are deposited on the surface to modify metal parts. A high-powered pulsed Nd:YAG laser is mostly used, emitting near infrared laser radiation to create a melt pool on a metallic substrate of interest. Pulsed lasers concentrate their output energy into brief high-power bursts. The laser beam is focused to a small spot by one or more lenses. Metal powders are pushed around the laser with a carrier gas or by gravity, and an inert gas is often used to shield the melt pool from atmospheric oxygen. By moving the plate on which the material of interest is placed, or the head of the laser, a nanoscale pattern of the material is deposited on the surface. By repetition of this process, 3D structures can be created. LENS has been used for net shape manufacturing to fabricate porous Ti structures for hard tissue replacement, but mostly for coatings of various metallic materials (**Figure 4**).[75–78]

Selective laser melting/sintering

SLS mostly uses a CO_2 high-heat laser to melt, sinter, or selectively fuse plastic, ceramic, metal, and glass powder particles. The particles can be fused layer by layer to form 3D structures. SLS is a type of additive manufacturing, meaning the item is built-up from materials into a final form. SLS also requires a computer model or description of the final piece. The heat from the laser fuses together powdered material by hitting it with very hot pulses. SLS allows the creation of parts with accurate detail with a structural resolution down to 30 μm.[79]

Laser interference lithography

A very promising technique for creating nanoscale surface patterns down to a 5 nm depth is laser interference lithography (LIL). LIL is a maskless lithographic technique using the

https://doi.org/10.1557/mrs.2011.273 Published online by Cambridge University Press

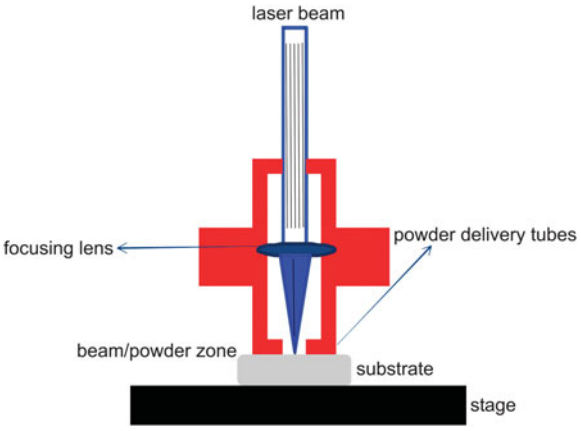


Figure 4. General scheme representing the laser engineered net shaping (LENS) process. LENS uses metal powders to create nanostructures, which are deposited on the surface to modify metal parts. A high-powered pulsed laser creates a melt pool on a metallic substrate of interest. The laser beam is focused to a small spot by one or more lenses. Metal powders are pushed around the laser with a carrier gas or just by gravity. By moving the plate on which the material of interest is placed, or the head of the laser, a pattern of the material is deposited on the surface.

interference pattern of two obliquely incident beams.[80,81] One part of the laser beam reaches a photoresist layer directly, while the second part of the laser reaches the photoresist layer via a mirror and produces a regular interference pattern in the photoresist, followed by etching. A line pattern is created using two lasers, whereas a dot type pattern can be created by using three lasers (two interfering beams).[82] By the use of an extra interference beam (four-beams in total), periodic arrays of holes are generated forming pillar-like structures.[83]

In vitro experiments using laser surface treatments

On the basis of their chemical properties, bone implant materials can roughly be divided into metals, ceramics, and polymers. These different material classes provide very different mechanical characteristics.[84] The mechanical properties of an implant biomaterial determine stress-strain, elasticity, tension-compression, shear, and fracture resistance properties.[85] Lasers have been used to modify the surfaces in all three main groups of materials. Although some studies report complete experimental laser conditions and parameters, unfortunately most do not give the complete experimental conditions necessary for good reproducibility. It must be emphasized, however, that a careful selection of laser parameters for surface modification is of primary importance. Thus, in the following paragraphs, we will discuss only the final results obtained with different materials and different types of cells.

Titanium and titanium alloys

Because of their good mechanical properties such as biocompatibility and corrosion resistance, titanium and titanium alloys are the most commonly used medical implant materials for bone tissue replacement in oral and orthopedic surgeries. The first laser surface treatment procedure on titanium was actually performed to join titanium structures in order to avoid severe embrittlement. Cracks normally appear while joining titanium structures when using an oxygen flame. Using tungsten gas as a laser source was shown to be a better heating substitute for the oxygen used.[86] Using a combination of several excimer laser treatments, Berezani et al. demonstrated that in titanium samples, the original alpha-titanium crystal structure was preserved,[87] whereas Sisti et al. demonstrated that such samples had better isomorphic characteristic, increased surface area, and micro-roughness.[88] In another study, using laser-based optical interference and direct laser melting techniques, microtexture features were produced on Ti-6Al-4V alloys. Subsequently, improved wettability and better cellular attachment were demonstrated when MC3T3-E1 osteoblast cells were used.[89] Similar results with improved proliferation rate were obtained with human osteosarcoma U2-OS cells seeded on Er,Cr:YSGG laser-treated titanium.[90]

Porosity and pore size of biomaterials play an important role in bone formation *in vivo*. Higher porosity and pore size result in greater bone ingrowth, implant stability, and better integration of the implant into the bone tissue. Using a direct Nd:G laser forming method on titanium, pores with a diameter of 300 μm were created, and it was shown that cells grew along the rims of the pores better than in the control samples.[91] Furthermore, using SLM, microporous titanium alloy implants created by the use of a Nd:YAG laser demonstrated very good mechanical stability. Thus lasers can be used for the purpose of bone ingrowth production or orthopedic devices.[92] Xue produced titanium porous implants using the LENS method and tested the implant with human osteoblast cells.[93] The results clearly demonstrated strong local adhesion, increased bone cell proliferation and differentiation, and an enhanced ECM formation compared to the non-treated controls. The results obtained also indicated that a critical pore size of 200 μm or higher was needed for cell in-growth into the pores. Below such dimensions, cells bridged the pore surface without any in-growth into the pores.

Cell interactions with laser-modified polymers and other materials

Different types of cells can be immobilized on a variety of biopolymers via covalent conjugation, hydrophobic interaction, or electrostatic interaction. Laser-modified polymer materials with nanoscale and micron-scale features produced on different types of polymers demonstrated improved grow rate, attachment, and differentiation of various type of cells. Surface KrF excimer laser irradiation on polystyrene significantly enhanced adhesion, alignment, and proliferation of human kidney cells (HEK-293) compared to unmodified controls.[94] Chinese hamster ovary (CHO-K1) cells and skeletal muscle cells aligned along the direction of the nanostructures, which had a periodicity between 200–430 nm and a depth of 30–100 nm. The alignment was only observed when the periodicity was above a critical value that was cell-type specific. Furthermore, using excimer laser irradiation on polyethylene terephthalate films

https://doi.org/10.1557/mrs.2011.273 Published online by Cambridge University Press

clearly revealed that laser treatment also improved the adhesion and proliferation of human embryonic epithelial cells.[95] The maximal ablation depth on the surface of films was 1 μm, and the cell number sharply increased reciprocal to the laser fluency.

The endothelium is the thin layer of cells that lines the interior surface of blood vessels. Using KrF excimer laser radiation, polyurethane films with micropores down to a size of 1 μm were produced to study endothelialization rates. Results showed that pore size and pore density were both important; the endothelization rate increased with an increasing pore size. The highest endothelialization was found on films with micropores between 18 and 50 μm in diameter.[96]

A typical neuron possesses a cell body, dendrites, and an axon. Dendrites are branching filaments that arise from the cell body, often extending for hundreds of micrometers, and an axon is a filament that arises from the cell body and can travel for distances as far as 1 m in humans.[97] Finding new strategies to improve neuronal cell growth is important to study neurogenesis more precisely. Adult rat neural progenitor cells were seeded on polyethersulfone fibers that were treated with a KrF excimer laser to create microchannels. The results showed spontaneous cell process growth into the channels of the scaffold wall, while preventing the entrance of cell bodies.[98]

Cones and ripples with spacings ranging from 2 to 25 μm were produced on poly(ethylene terephthalate) films by UV laser ablation to study the response of the shape and spacing of surface features on fibroblasts. Here, the highest cell attachment was observed in the regions with cones at ~4 μm spacing. As feature spacing increased, cell spreading decreased, and the fibroblasts became more circular, indicating stress-mediated cell shrinkage.[99] In another study, fibroblasts and endothelial cells initially proliferated better on polymer nylon 12 films treated with an excimer laser.[100] Similar results were obtained on micron-scale structures generated on polyamide Kapton using an ArF excimer laser. Moreover, the same technique could be employed with a phase mask to generate nanoscale features.[101]

Using LIL, recently we studied the response of osteoblast-like cells to nanogrooved polystyrene substrates and demonstrated that cells aligned down to groove widths of 75 nm and depths of 35 nm. In addition, the study demonstrated that ECM produced by osteoblasts was sensitive to even smaller nanopatterns, and specific gene expression was induced by the nanopatterns (**Figure 5**).[102]

In vivo studies using laser surface treatments

Pre-clinical development is a stage of research that begins before clinical trials (testing in humans) can begin, and during which important feasibility, testing, and safety are investigated in animal models. The success of bone but also other implants depends on better tissue-material interactions, as it improves the fixation of the implant to the bone. Thus, *in vivo* pre-clinical studies are very important to investigate the behavior of the implants and its fixation before real clinical studies are done. Until now, very few pre-clinical and clinical studies have been performed with laser-treated implants. In this section, we will discuss some of the results obtained so far.

Surface modification of titanium machined implants, which were additionally etched with a laser and micro-arc oxidation (plasma-electrochemical process), showed enhanced bone formation versus that seen around machined titanium implants in rabbits.[103] In another study, low-level laser radiation improved the bone healing response around a titanium dental implant in the tibia of rabbits, but only after 45 days of implantation.[104] In another similar study with a longer implantation period (six months), titanium machined implants, partly modified with nanofeatures by Nd:YAG laser irradiation, were implanted in the femurs and tibias of rabbit models and investigated.

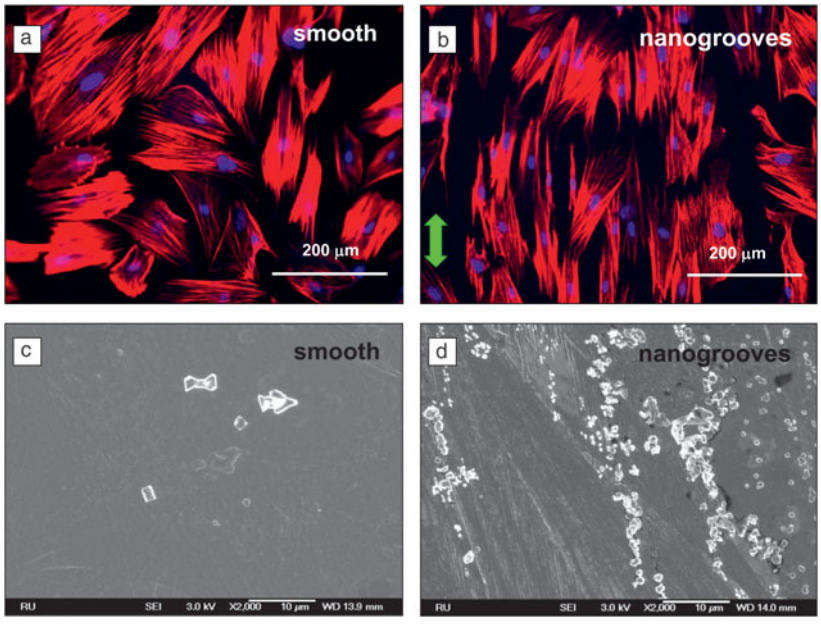


Figure 5. Fluorescent micrographs of cytoskeleton actin filaments staining (red) and nucleus staining (blue) of osteoblast-like cells grown for 48 h on a smooth and nanogrooved polystyrene substrate. Nanotextured groove patterns were made using laser interference lithography (LIL) on silica. Polystyrene replicas were made by solvent casting. In this study, patterned wafers with 130 nm wide grooves (200 nm pitch) and a depth of ~50 nm were used. (a) Cells grown on the smooth substrate have random cell and actin orientation. (b) Note that cells and actin filaments oriented in parallel direction toward the nanogrooves. The green arrow indicates the direction of the nanogrooves. (c–d) Scanning electron microscopy micrographs of osteoblast-like cells after eight days of cell culture. Note that the calcium particles on top of the cells are found more on the nanogrooved substrate when compared to the smooth substrate and orient parallel to the groove direction.

https://doi.org/10.1557/mrs.2011.273 Published online by Cambridge University Press

Good osseointegration of the implant in bone was observed for both implant types. The partly laser-modified titanium implants were associated with an increased removal torque after six months compared to the machined titanium implants. A different failure pattern with fractures in the bone tissue rather than at the bone implant interface also suggested better bone bonding than laser-modified surfaces.[105]

Ethylene-propylene rubber (EPR)-based materials that were chemically etched, followed by CO_2-pulsed laser treatment, implanted in the deep intramuscular and peritoneal layers (the lining of the abdominal cavity) in rabbits, showed that after eight weeks of implantation, the adhesion of the macrophages to the chemically modified laser-treated EPR samples was significantly lower than their adhesion on the unmodified surfaces. Also, no acute or chronic inflammatory reaction was observed at the site of implantation, and a thinner fibrous tissue capsule formed around the modified samples, whereas foreign body giant cells adhered to unmodified EPR.[106]

Porous Ti6A14V alloy implants fabricated by LENS and implanted into the femurs of rabbits demonstrated that new bone penetrated into the pores and directly bonded to the walls. This was seen together with a significant increase in calcium within the implants, indicating excellent biological tissue ingrowth through the interconnected porosity when compared with the controls.[107]

The inflammatory process induced by implant surfaces is an important component of the tissue response, where knowledge is limited regarding the role of surface topography. Palmquist et al. showed that the combination of surface micro- and nano-features on laser-treated titanium implants contributes to the down-regulation of early inflammatory events. The machined and laser-treated implants were implanted subcutaneously in rats for 72 hours. The results revealed that significantly fewer inflammatory cells were attracted to the sites with the laser-modified implants compared with machined titanium implants.[108]

Clinical trials

After a tooth extraction, resorption of the crestal bone (i.e, beneath the tooth) can occur. By placing an implant, this process can be reduced. Tapered 2 mm dental implants treated with Laser-Lok (LL) microchannels were compared to machined (control) implants of the same design after implantation in the crestal bone of 15 patients. LL limited the bone loss to 0.59 mm as opposed to the 1.94 mm crestal bone loss reported for control implants.[109]

Recent studies using direct laser metal sintering (DLMS) were used for mandibular reconstruction. Implantation of titanium meshes treated with DLMS in four patients showed that it can produce structures with complex geometry and consequently allow better osteoconductive properties (new bone formation). After eight weeks, the results showed a newly formed tissue composed of calcium and phosphorus. Good bone-to-implant contact was observed, as the bone-to-implant contact presented a mean of 60.5±11.6%.[110]

Taken together, the pre-clinical and clinical studies using LSE for micro- or nanoscale surface topographical features indicate that structured surfaces promote long-term bone bonding and interfacial strength. However, more *in vivo* studies are needed to investigate other mentioned biomaterials. In addition, studies comparing implants treated with different techniques need to be taken into account to find the best candidates.

Summary

The advantages of using laser techniques for texturing surfaces over other conventional methods (chemical etching, anodization) are that they are rapid and extremely clean, focus great amounts of energy in one spot for a short time (pulse), and generate complex nano-features with high resolution. Unlike the different lithographic techniques, which require time-consuming steps such as class 100 clean rooms, spin coaters, vacuum chambers, and optimization protocols to coat and develop specific photoresists or thin films, laser-based techniques can avoid them and shorten these steps. The laser techniques can be used to selectively modify surface composition and microstructures without affecting the surrounding material properties or causing serious thermal distortion. The efficiency of absorption is linked to both the physical state of the material and the power density at the surface. As expected, higher power density is required to vaporize rather than to melt the material. Because of their ability to show no, or very little, thermal effects, excimer laser beams with higher density are particularly suited to photoablation. However, a laser beam with sufficient energy density has a limited beam size. Therefore, laser surface melting is less efficient than other conventional methods such as thermal spraying, in terms of coverage rate. Most laser surface engineering (LSE) processes appear expensive compared to other technologies; still, in many cases, they can be adapted to be more cost-effective because of their precision and speed.

Studies done on the effects of micro- and nano-textures on cell biocompatibility using conventional methods have shown good results in the last 30 years, particularly with regard to cellular attachment, proliferation, and differentiation of cells. LSE has just recently shown that the same effect can be achieved and gave the same biocompatibility effects. Pre-clinical and clinical studies with micro- and nanoscale laser engineered surface structures still need to be done. By understanding how physical surface parameters influence cellular attachment or how to develop a direct single-step method for creating micron or nanoscale surface texture, we can more effectively design biomaterial surfaces for a variety of tissue engineering applications.

References

1. J.B. Park, R.S. Lakes, *Biomaterials: Introduction* (Springer, NY, 3rd edition), 2007.
2. C.H. Townes, *Nature* **447**, 654 (2007).
3. K. Nakashima, X. Zhou, G. Kunkel, Z. Zhang, J.M. Deng, R.R. Behringer, B. de Crombrugghe, *Cell* **108**, 17 (2002).
4. B. Chehroudi, T.R. Gould, D.M. Brunette, *J. Biomed. Mater. Res.* **23**, 1067 (1989).
5. H. Shin, S. Jo, A.G. Mikos, *Biomaterials* **24**, 4353 (2003).

https://doi.org/10.1557/mrs.2011.273 Published online by Cambridge University Press

6. J.M. Anderson, A. Rodriguez, D.T. Chang, *Semin. Immunol.* **20**, 86 (2008).
7. P. Roach, D. Eglin, K. Rohde, C.C. Perry, *J. Mater. Sci. Mater. Med.* **18**, 1263 (2007).
8. J.M. Anderson, B.D. Ratner, A.S. Hoffman, F.J. Schoen, J.E. Lemons, in *Biomaterial Science: An Introduction to Materials in Medicine*, Eds. (Elsevier Academic Press, San Diego, 2004), vol. **2**, pp. 296–304.
9. J.M. Anderson, *Annu. Rev. Mater. Res.* **31**, 81 (2001).
10. B.D. Ratner, *J. Dent. Educ.* **65**, 1340 (2001).
11. T. Albrektsson, L. Sennerby, *Int. J. Prosthodont.* **3**, 30 (1990).
12. F. Rupp, L. Scheideler, N. Olshanska, M. de Wild, M. Wieland, J. Geis-Gerstorfer, *J. Biomed. Mater. Res. A* **76**, 323 (2006).
13. T. Albrektsson, P.I. Branemark, H.A. Hansson, B. Kasemo, K. Larsson, I. Lundstrom, D.H. McQueen, R. Skalak, *Ann. Biomed. Eng.* **11**, 27 (1983).
14. B.D. Ratner, *Ann. Biomed. Eng.* **11**, 313 (1983).
15. B. Kasemo, *J. Prosthet. Dent.* **49**, 832 (1983).
16. A.F. von Recum, T.G. van Kooten, *J. Biomater. Sci., Polym. Ed.* **7**, 181 (1995).
17. L. Le Guehennec, A. Soueidan, P. Layrolle, Y. Amouriq, *Dent. Mater.* **23**, 844 (2007).
18. D. Williams, *Biomaterials* **29**, 1737 (2008).
19. E. Palin, H.N. Liu, T.J. Webster, *Nanotechnology* **16**, 1828 (2005).
20. P.T. de Oliveira, A. Nanci, *Biomaterials* **25**, 403 (2004).
21. Y.W. Fan, F.Z. Cui, S.P. Hou, Q.Y. Xu, L.N. Chen, I.S. Lee, *J. Neurosci. Methods* **120**, 17 (2002).
22. T.J. Webster, R.W. Siegel, R. Bizios, *Nanostruct. Mater.* **12**, 983 (1999).
23. M.L. Pantoya, J.J. Granier, *Propellants Explos. Pyrotech.* **30**, 53 (2005).
24. T.J. Webster, J.U. Ejiofor, *Biomaterials* **25**, 4731 (2004).
25. S.G. Zhang, *Biotechnol. Adv.* **20**, 321 (2002).
26. M. Park, C. Harrison, P.M. Chaikin, R.A. Register, D.H. Adamson, *Science* **276**, 1401 (1997).
27. J.J. Norman, T.A. Desai, *Ann. Biomed. Eng.* **34**, 89 (2006).
28. A. Senefelder, *The Invention of Lithography* (Kessinger Publishing, Montana, 1911).
29. M. Altissimo, *Biomicrofluidics*, 4 (2010).
30. Y. Chen, A. Pepin, *Electrophoresis* **22**, 187 (2001).
31. A.A. Tseng, *Small* **1**, 924 (2005).
32. A.J. Torres, M. Wu, D. Holowka, B. Baird, *Annu. Rev. Biophys.* **37**, 265 (2008).
33. S.Y. Chou, P.R. Krauss, P.J. Renstrom, *Appl. Phys. Lett.* **67**, 3114 (1995).
34. M.D. Austin, H.X. Ge, W. Wu, M.T. Li, Z.N. Yu, D. Wasserman, S.A. Lyon, S.Y. Chou, *Appl. Phys. Lett.* 84 (2004).
35. L. Prodanov, J. te Riet, E. Lamers, M. Domanski, R. Luttge, J.J. van Loon, J.A. Jansen, X.F. Walboomers, *Biomaterials* **31**, 7758 (2010).
36. A.S. Curtis, B. Casey, J.O. Gallagher, D. Pasqui, M.A. Wood, C.D. Wilkinson, *Biophys. Chem.* **94**, 275 (2001).
37. M.J. Dalby, S.J. Yarwood, M.O. Riehle, H.J. Johnstone, S. Affrossman, A.S. Curtis, *Exp. Cell Res.* **276**, 1 (2002).
38. T.J. Webster, R.W. Siegel, R. Bizios, *Biomaterials* **20**, 1221 (1999).
39. T.J. Webster, C. Ergun, R.H. Doremus, R.W. Siegel, R. Bizios, *Biomaterials* **21**, 1803 (2000).
40. T.J. Webster, C. Ergun, R.H. Doremus, R.W. Siegel, R. Bizios, *J. Biomed. Mater. Res.* **51**, 475 (2000).
41. T.J. Webster, T.A. Smith, *J. Biomed. Mater. Res. A* **74**, 677 (2005).
42. R.L. Price, L.G. Gutwein, L. Kaledin, F. Tepper, T.J. Webster, *J. Biomed. Mater. Res. A* **67**, 1284 (2003).
43. H. Liu, E.B. Slamovich, T.J. Webster, *J. Biomed. Mater. Res. A* **78**, 798 (2006).
44. A.J. Dulgar-Tulloch, R. Bizios, R.W. Siegel, *J. Biomed. Mater. Res. A* **90**, 586 (2009).
45. M.J. Dalby, S. Childs, M.O. Riehle, H.J. Johnstone, S. Affrossman, A.S. Curtis, *Biomaterials* **24**, 927 (2003).
46. M.J. Dalby, M.O. Riehle, D.S. Sutherland, H. Agheli, A.S. Curtis, *Biomaterials* **25**, 77 (2004).
47. M.J. Dalby, G.E. Marshall, H.J. Johnstone, S. Affrossman, M.O. Riehle, *IEEE Trans. Nanobiosci.* **1**, 18 (2002).
48. M.J. Dalby, M.O. Riehle, H. Johnstone, S. Affrossman, A.S. Curtis, *Biomaterials* **23**, 2945 (2002).
49. M.J. Dalby, M.O. Riehle, H. Johnstone, S. Affrossman, A.S. Curtis, *Cell Biol. Int.* **28**, 229 (2004).
50. M.J. Dalby, M.O. Riehle, H.J. Johnstone, S. Affrossman, A.S. Curtis, *Tissue Eng.* **8**, 1099 (2002).
51. M.J. Dalby, D. McCloy, M. Robertson, H. Agheli, D. Sutherland, S. Affrossman, R.O. Oreffo, *Biomaterials* **27**, 2980 (2006).
52. M.J. Dalby, C.C. Berry, M.O. Riehle, D.S. Sutherland, H. Agheli, A.S. Curtis, *Exp. Cell Res.* **295**, 387 (2004).
53. M.J. Dalby, M.O. Riehle, D.S. Sutherland, H. Agheli, A.S. Curtis, *J. Biomed. Mater. Res. A* **69**, 314 (2004).
54. M.J. Dalby, M.O. Riehle, D.S. Sutherland, H. Agheli, A.S. Curtis, *Biomaterials* **25**, 5415 (2004).
55. M.J. Biggs, R.G. Richards, N. Gadegaard, R.J. McMurray, S. Affrossman, C.D. Wilkinson, R.O. Oreffo, M.J. Dalby, *J. Biomed. Mater. Res. A* (2008).
56. M.J. Biggs, R.G. Richards, N. Gadegaard, C.D. Wilkinson, M.J. Dalby, *J. Mater. Sci. Mater. Med.* **18**, 399 (2007).
57. M.J. Biggs, R.G. Richards, N. Gadegaard, C.D. Wilkinson, M.J. Dalby, *J. Orthop. Res.* **25**, 273 (2007).
58. M.J. Dalby, N. Gadegaard, R. Tare, A. Andar, M.O. Riehle, P. Herzyk, C.D. Wilkinson, R.O. Oreffo, *Nat. Mat.* **6**, 997 (2007).
59. M.J. Dalby, N. Gadegaard, C.D. Wilkinson, *J. Biomed. Mater. Res. A* **84**, 973 (2008).
60. W.A. Loesberg, J. te Riet, F.C. van Delft, P. Schon, C.G. Figdor, S. Speller, J.J. van Loon, X.F. Walboomers, J.A. Jansen, *Biomaterials* **28**, 3944 (2007).
61. E. Lamers, R. van Horssen, J. te Riet, F.C. van Delft, R. Luttge, X.F. Walboomers, J.A. Jansen, *European Cells & Materials* **20**, 329 (2011).
62. S. Lenhert, M.B. Meier, U. Meyer, L.F. Chi, H.P. Wiesmann, *Biomaterials* **26**, 563 (2005).
63. C.S. Chen, M. Mrksich, S. Huang, G.M. Whitesides, D.E. Ingber, *Science* **276**, 1425 (1997).
64. A.A. Oliva Jr., C.D. James, C.E. Kingman, H.G. Craighead, G.A. Banker, *Neurochem. Res.* **28**, 1639 (2003).
65. M. Scholl, C. Sprossler, M. Denyer, M. Krause, K. Nakajima, A. Maelicke, W. Knoll, A. Offenhausser, *J. Neurosci. Methods* **104**, 65 (2000).
66. D.K. Hoover, E.J. Lee, M.N. Yousaf, *Langmuir* **25**, 2563 (2009).
67. G. Giavaresi, M. Tschon, J.H. Daly, J.J. Liggat, D.S. Sutherland, H. Agheli, M. Fini, P. Torricelli, R. Giardino, *J. Biomater. Sci. Polym.* **17**, 1405 (2006).
68. K.C. Popat, L. Leoni, C.A. Grimes, T.A. Desai, *Biomaterials* **28**, 3188 (2007).
69. V.V. Semak, N.B. Dahotre, *Surface Engineering Series* 35 (1998).
70. F.J. Duarte, *Tunable Lasers Handbook* (Academic Press, NY, 1995).
71. H. Injeyan, G. Goodno, *High Power Laser Handbook* (McGraw-Hill, NJ, 2011).
72. L.E. Probst, *Int. Ophthalmol. Clin.* **48**, 9 (2008).
73. A. Kurella, N.B. Dahotre, *J. Biomater. Appl.* **20**, 5 (2005).
74. R. Asthana, A. Kumar, N.B. Dahotre, *Materials Processing and Manufacturing Science* (Elsevier, NY, 2006).
75. S.R. Paital, Z. Cao, W. He, N.B. Dahotre, *Biofabrication* **2**, 025001 (2010).
76. V.K. Balla, S. Banerjee, S. Bose, A. Bandyopadhyay, *Acta Biomater.* **6**, 2329 (2010).
77. V.K. Balla, P.D. DeVasConCellos, W. Xue, S. Bose, A. Bandyopadhyay, *Acta Biomater.* **5**, 1831 (2009).
78. B.V. Krishna, S. Bose, A. Bandyopadhyay, *J. Biomed. Mater. Res. Part B* **89B**, 481 (2009).
79. I. Yadroitsev, *Selective Laser Melting* (LAP Lambert Academic Publishing, UK, 2010).
80. F.J. van Soest, H.A.G.M. van Wolferen, H.J.W.M. Hoekstra, R.M. de Ridder, K. Worhoff, P.V. Lambeck, *Jpn. J. Appl. Phys., Part 1* **44**, 6568 (2005).
81. R. Luttge, *J. Phys. D: Appl. Phys.* **42**, 18 (2009).
82. A.F. Lasagni, D.F. Acevedo, C.A. Barbero, F. Mucklich, *Adv. Eng. Mater.* **9**, 99 (2007).
83. C. Tan, C.S. Peng, J. Pakarinen, M. Pessa, V.N. Petryakov, Y.K. Verevkin, J. Zhang, Z. Wang, S.M. Olaizola, T. Berthou, S. Tisserand, *Nanotechnology* **20**, 125303 (2009).
84. F.W. Cooke, *Biomaterial Science: An Introduction to Materials in Medicine*, **2**, 23 (2004).
85. G. Binyamin, B.M. Shafi, C.M. Mery, *Semin. Pediatr. Surg.* **15**, 276 (2006).
86. R.R. Wang, G.E. Welsch, *J. Prosthet. Dent.* **74**, 521 (1995).
87. M. Bereznai, I. Pelsoczi, Z. Toth, K. Turzo, M. Radnai, Z. Bor, A. Fazekas, *Biomaterials* **24**, 4197 (2003).
88. K.E. Sisti, I.R. Garcia Jr., A.C. Guastaldi, A.C. Antoniolli, R. Rossi, L. Brochado, Neto Ade, *Acta cirurgica brasileira/Sociedade Brasileira para Desenvolvimento Pesquisa em Cirurgia* **21** (Suppl. 4), 57 (2006).
89. S.R. Paital, W. He, C. Daniel, N.B. Dahotre, *JOM Journal of the Minerals, Metals and Materials Society* **62**, 76 (2010).
90. H.H. Huang, Y.C. Chuang, Z.H. Chen, T.L. Lee, C.C. Chen, *Dent. Mater.* **23**, 410 (2007).
91. L. Mullen, R.C. Stamp, W.K. Brooks, E. Jones, C.J. Sutcliffe, *J. Biomed. Mater. Res. Part B* **89B**, 325 (2009).
92. C.Y. Lin, T. Wirtz, F. LaMarca, S.J. Hollister, *J. Biomed. Mater. Res. Part A* **83**, 272 (2007).
93. W. Xue, B.V. Krishna, A. Bandyopadhyay, S. Bose, *Acta Biomater.* **3**, 1007 (2007).
94. E. Rebollar, I. Frischauf, M. Olbrich, T. Peterbauer, S. Hering, J. Preiner, P. Hinterdorfer, C. Romanin, J. Heitz, *Biomaterials* **29**, 1796 (2008).
95. G. Mayer, N. Blanchemain, C. Dupas-Bruzek, V. Miri, M. Traisnel, L. Gengembre, D. Derozier, H.F. Hildebrand, *Biomaterials* **27**, 553 (2006).
96. T. Matsuda, Y. Nakayama, *J. Biomed. Mater. Res.* **31**, 235 (1996).
97. R.S. Nowakowski, *Proceedings of the National Academy of Sciences of the United States of America* **103**, 12219 (2006).
98. G. Mapili, Y. Lu, S. Chen, K. Roy, *J. Biomed. Mater. Res. Part B* **75**, 414 (2005).

https://doi.org/10.1557/mrs.2011.273 Published online by Cambridge University Press

99. P. Chandra, K. Lai, H.J. Sung, N.S. Murthy, J. Kohn, *Biointerphases* **5**, 53 (2010).
100. M.D. Ball, R. Sherlock, T. Glynn, *J. Mater. Sci. Mater. Med.* **15**, 447 (2004).
101. M.D. Ball, U. Prendergast, C. O'Connell, R. Sherlock, *Exp. Mol. Pathol.* **82**, 130 (2007).
102. E. Lamers, X. Frank Walboomers, M. Domanski, J. te Riet, F.C. van Delft, R. Luttge, L.A. Winnubst, H.J. Gardeniers, J.A. Jansen, *Biomaterials* **12**, 3307 (2010).
103. Z. Guo, L. Zhou, M. Rong, A. Zhu, H. Geng, *Int. J. Oral Maxillofac. Implants* **25**, 130 (2010).
104. C.B. Lopes, A.L. Pinheiro, S. Sathaiah, J. Duarte, M. Cristinamartins, *Photomed. Laser Surg.* **23**, 27 (2005).
105. A. Palmquist, L. Emanuelsson, R. Branemark, P. Thomsen, *J. Biomed. Mater. Res. Part B* **97**, 289 (2011).
106. H. Mirzadeh, A.A. Katbab, M.T. Khorasani, R.P. Burford, E. Gorgin, A. Golestani, *Biomaterials* **16**, 641 (1995).
107. A. Bandyopadhyay, F. Espana, V.K. Balla, S. Bose, Y. Ohgami, N.M. Davies, *Acta Biomaterialia* **6**, 1640 (2010).
108. A. Palmquist, A. Johansson, F. Suska, R. Brånemark, P. Thomsen, *Clin. Implant Dent. Relat. Res.* **97**, 289 (2011).
109. G.E. Pecora, R. Ceccarelli, M. Bonelli, H. Alexander, J.L. Ricci, *Implant Dent.* **18**, 57 (2009).
110. C. Mangano, A. Piattelli, M. Raspanti, F. Mangano, A. Cassoni, G. Iezzi, J.A. Shibli, *Lasers Medical Science* **26**, 133 (2010). □

ACNS 2012

American Conference on Neutron Scattering
June 24-28, 2012 | Georgetown University Hotel and Conference Center
Washington, D.C., USA

CALL FOR PAPERS

SAVE THE DATE

Join us for the sixth American Conference on Neutron Scattering (ACNS 2012). Hosted at historic Georgetown University in Washington, D.C., the conference will provide essential information on the breadth and depth of current neutron-related research worldwide. This year's conference will feature a combination of invited and contributed talks, posters sessions, tutorials and an industrial exhibit. Plus, the last day of the conference features a tour of NIST Center for Neutron Research. Mark your calendars today and plan to attend ACNS 2012!

SCIENTIFIC PROGRAM

The four-day conference will feature oral and poster presentations covering:

- Plenary and Prize sessions (Invited Speakers ONLY)
- Sources, Instrumentation and Software
- Soft Condensed Matter
- Hard Condensed Matter
- Biology
- Chemistry
- Energy and Engineering Applications
- Neutron Physics

CONFERENCE VENUE

Georgetown, situated on the bluffs of Washington, D.C., is rich in history and culture, making it an ideal conference and vacation destination. Known for its high-end shopping and dining and quaint row houses overlooking Waterfront Harbor, Georgetown is truly unlike any other city in the U.S. Take a walk back in time on Georgetown's famous 18th century cobblestone streets. Visit the palatial gardens at Dumbarton Oaks, a mansion built in 1800 for Senator John Calhoun. Add in all the sites and attractions found in nearby Washington, D.C., and you'll never have a dull moment!

For the most up-to-date information on ACNS 2012, visit **www.mrs.org/acns-2012**

OFFICIAL SPONSOR

Neutron Scattering Society of America (NSSA)

CONFERENCE HOST

NIST Center for Neutron Research

IMPORTANT DATES

Abstract Submission Opens
January 16, 2012

Preregistration Opens
Early April

Abstract Submission Ends
April 2, 2012

CONFERENCE CHAIRS

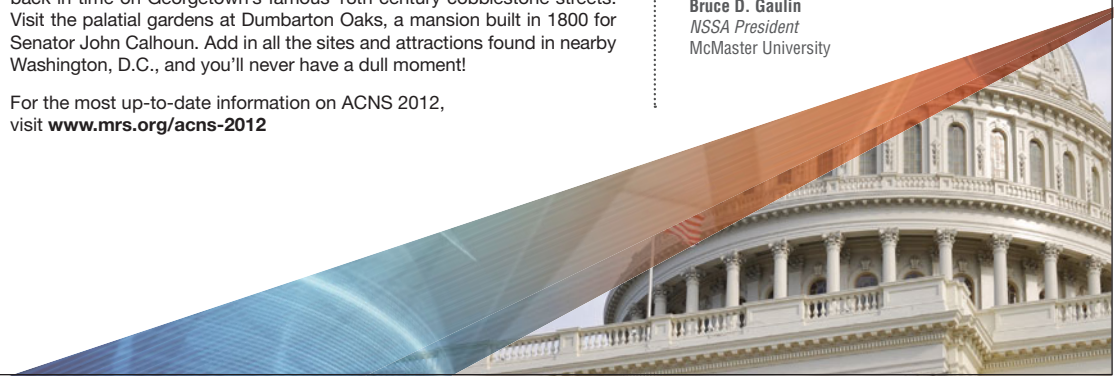
Julie Borchers
Organizing Committee Conference Chair
NIST Center for Neutron Research

Nitash Balsara
Program Committee Co-Chair
University of California, Berkeley

Stephan Rosenkranz
Program Committee Co-Chair
Argonne National Laboratory

Susan Krueger
Local Organizing Committee Conference Chair
NIST Center for Neutron Research

Bruce D. Gaulin
NSSA President
McMaster University



https://doi.org/10.1557/mrs.2011.273 Published online by Cambridge University Press